Journal of Neuropathology and Experimental Neurology

Vol. 58, No. 8
August, 1999
pp. 815–824

Accumulation of Intracellular Amyloid-β Peptide (Aβ 1-40) in Mucopolysaccharidosis Brains

STEPHEN D. GINSBERG, PHD, JAMES E. GALVIN, MD, MSC, VIRGINIA M-Y LEE, PHD, LUCY B. RORKE, MD, DENNIS W. DICKSON, MD, JOHN H. WOLFE, VMD, PHD, MARGARET Z. JONES, MD, AND JOHN Q. TROJANOWSKI, MD, PHD

Abstract. To evaluate whether in vivo accumulations of heparan sulfate caused by inborn errors in the metabolism of glycosaminoglycans lead to the formation of neurofibrillary tangles and/or senile plaques, as seen in Alzheimer disease (AD), we studied postmortem brains from 9 patients, ages 1 to 42 years, with mucopolysaccharidosis (MPS). The brains of patients with Hurler's syndrome (MPS I; n = 5) and Sanfilippo's syndrome (MPS III; n = 4) as well as from caprine MPS IIID and murine MPS VII models were evaluated by thioflavine-S staining and by immunohistochemistry using antibodies directed against heparan sulfate proteoglycans, hyperphosphorylated tau, amyloid-β peptide precursor proteins (APP), and amyloid-β peptides (Aβ [1-40], and Aβ [1-42]). A two-site sandwich enzyme-linked immunosorbent assay (ELISA) was also utilized to compare levels of total soluble and insoluble Aβ (1-40) and Aβ (1-42) obtained from temporal cortex of MPS patients. Although no neurofibrillary tangles, senile plaques, or tau-positive lesions were detected in any of the MPS brains studied here, antibodies directed against Aβ (1-40) intensely and diffusely stained the cytoplasm of cells throughout the brains of the MPS patients and the caprine MPS model. The ELISA assay also demonstrated a significant 3-fold increase in the level of soluble Aβ (1-40) in the MPS brains compared with normal control brains. Thus, at least some of the metabolic defects that lead to accumulations of glycosaminoglycans in MPS also are associated with an increase in immunoreactive Aβ (1-40) within the cytoplasmic compartment where they could contribute to the dysfunction and death of affected cells in these disorders, but not induce the formation of plaques and tangles. Models of MPS may enable mechanistic studies of the role Aβ and glycosaminoglycans play in the amyloidosis that is a neuropathological feature of AD.

Key Words: Amyloid-β peptides; Glycosaminoglycans; Heparan sulfate proteoglycan; Neurofibrillary tangles; Senile plaques; Tau protein.

INTRODUCTION

Neurofibrillary tangles (NFTs) consisting primarily of paired helical filaments (PHFs), and senile plaques (SPs) comprised predominantly of amyloid fibrils, are the pathological hallmarks of Alzheimer disease (AD) and related neurodegenerative disorders (1–3). In vitro studies have demonstrated that hyperphosphorylated tau (PHFtau) can self-aggregate into fibrillar polymers that resemble PHFs and straight filaments (4–10). The region of tau that is necessary for polymerization consists of the microtubule-binding domain (11, 12), and PHF formation is believed to hamper the binding of tau to microtubules, leading to microtubule disassembly, loss of axonal transport, and subsequent neuronal degeneration (13). Amyloid-β peptides (Aβ), the major constituent of amyloid fibrils in SPs (14, 15), also self-aggregate into filaments under appropriate in vitro conditions (16–20). Aβ terminating at amino acid residue 42 (Aβ [1-42]) is deposited initially in SPs, and aggregates at a faster rate than the more soluble Aβ terminating at amino acid residue 40 (Aβ [1-40]) (21–24). However, the in vivo mechanism(s) by which tau and Aβ aggregate, form insoluble deposits, and lead to AD remain unknown.

Although self-aggregation of recombinant tau and Aβ has been demonstrated, nonphysiological quantities of these peptides are necessary for polymerization (9, 12, 25). Therefore, other molecules have been hypothesized to function as pathological chaperones to facilitate fibril formation. Recent studies suggest that pathological chaperones involved in PHF and amyloid fibril formation may include sulfated glycosaminoglycans (GAGs), notably heparan sulfate (HSGAG) and its most sulfated form, heparin (25–32). GAGs, or mucopolysaccharides, are sugar moieties that are bound to a protein core to form proteoglycans (i.e. heparan sulfate proteoglycan [HSPG]), molecules found in the extracellular matrix and basement membranes (33, 34). HSPGs and HSGAGs have been observed in association with NFTs in the AD brain (27, 29, 31). Moreover, HSPGs stimulate tau phosphorylation by several protein kinases (35, 36), and promote PHF formation from recombinant tau proteins in vitro under near physiologic concentrations (25–27, 32, 37). Similarly, HSPGs and HSGAGs have been observed

From the Center for Neurodegenerative Disease Research and Department of Pathology and Laboratory Medicine (SDG, JEG, VM-YL, JQT), University of Pennsylvania School of Medicine, Department of Neurology (JEG), MCP Hahnemann University, Department of Pathology (LBR), The Children's Hospital of Philadelphia, Department of Pathobiology (JHW), University of Pennsylvania School of Veterinary Medicine, Philadelphia, Pennsylvania; Mayo Clinic (DWD), Jacksonville, Florida; and Department of Pathology (MZJ), Michigan State University, East Lansing, Michigan.

Correspondence to: John Q. Trojanowski, MD, PhD, Center for Neurodegenerative Disease Research, Department of Pathology and Laboratory Medicine, University of Pennsylvania School of Medicine, 3rd Floor HUP-Maloney Bldg., 3600 Spruce St., Philadelphia, PA 19104-4283.

This work was supported by grants from the N.I.H. Several human brain tissues were obtained from the Brain and Tissue Bank for Developmental Disorders at the University of Maryland and University of Miami through NICHD contract #N01-HD-8-3284.

in association with SPs in AD brains (31, 38, 39), bind to the amyloid-β peptide precursor protein (APP) and Aβ in vitro, and accelerate Aβ fibril formation and stability (28, 30, 40–42).

To test the hypothesis that the accumulation of HSGAGs due to metabolic defects in vivo may lead to the formation of NFTs and/or SPs, we examined sections from the brains of subjects with autosomal recessive mucopolysaccharidosis (MPS), including MPS I and MPS III syndromes in which specific lysosomal hydrolase deficiencies lead to the accumulation of HSGAGs (43, 44). HSGAGs are the sole uncatabolized substrates in MPS III, whereas HSGAGs accumulate along with dermatan sulfate in MPS I. Tissue sections were evaluated by thioflavine-S (TS) staining and by immunohistochemistry using antibodies specific for HSPGs, PHFtau, APP, and Aβ. In addition, caprine (MPS IIID; a genetic disease in which goats are deficient in activity of N-acetylglucosamine 6-sulfatase]) (45) and murine (MPS VII; an hereditary disease in which homozygous mice are β-glucuronidase deficient]) (46) models of MPS also were evaluated for evidence of tangle and plaque pathology using the same methodology. A two-site sandwich enzyme-linked immunosorbent assay (ELISA) was utilized to compare levels of total soluble (extracted in Tris-buffered saline [TBS]) and insoluble (extracted in formic acid) Aβ (1-40) and Aβ (1-42) obtained from tissue homogenates of temporal neocortex of MPS, normal control, and AD brains. This previously characterized ELISA for soluble and insoluble Aβ (1-40) and Aβ (1-42) (47–51) allows for quantitative analysis of even small amounts (e.g. <100 pmol/g wet tissue) of Aβ (1-40) and Aβ (1-42) due to the specificity of the monoclonal antibodies (MAbs) used for the ELISA.

TABLE 1
Summary of Cases

Case No.	Diagnosis	Gender	Age	PMI	Brain Wt.	Fixation
1	MPS I	M	2.5	48	1,260	NBF
2	MPS I	M	6	48	1,250	NBF
3	MPS I	M	6	1.5	1,050	NBF
4	MPS I	F	6.5	2	*	NBF/F
5	MPS I	M	42	3	*	NBF/F
6	MPS III	F	1	12	*	NBF/F
7	MPS III	F	16	6	600	NBF
8	MPS III	M	14	4	*	NBF
9	MPS III	M	34	8	1,030	EtOH/F
10	GAU	F	6	12	790	NBF
11	NCL	F	5	4	660	NBF/F
12	NCL	*	*	6	1,110	F
13	NCL	M	6	20	*	NBF
14	CTR	M	19	16.5	1,500	NBF
15	CTR	M	62	5	1,360	EtOH/F
16	CTR	M	24	15	1,410	F
17	CTR	F	36	6	1,280	EtOH/F
18	CTR	M	71	13	1,300	EtOH/F
19	CTR	F	92	9	1,090	EtOH
20	AD	F	72	4.5	1,220	EtOH/F
21	AD	M	88	9	1,380	EtOH
22	AD	M	87	7	1,220	EtOH
23	AD	M	79	4	980	EtOH/F
24	AD	M	81	16.5	1,340	EtOH/F
25	AD	M	89	14	1,100	EtOH/F
26	DS	M	58	13	910	EtOH
27	DS	F	53	9	1,100	EtOH/F
28	DS	F	64	5	630	NBF/F
29	DS	F	67	16.5	1,080	EtOH/F

Abbreviations: AD = Alzheimer disease; CTR = control subjects; DS = Down syndrome; EtOH = 70% ethanol plus 150 mM NaCl; F = fresh-frozen tissue; Gau = Gaucher's syndrome; MPS I = Hurler's syndrome; MPS III = Sanfilippo's syndrome; NBF = 10% neutral buffered formalin; NCL = neuronal ceroid lipofuscinosis; PMI = postmortem interval; wt = weight in grams; * = data not available.

MATERIALS AND METHODS

Postmortem brain samples from neocortex, hippocampal formation, cerebellum, and striatum were obtained (n = 9 MPS; n = 6 normal controls [CTR]; disease controls: n = 3 neuronal ceroid lipofuscinosis [NCL]; n = 1 Gaucher's disease; n = 6 AD; n = 4 Down syndrome [DS]; [Table 1]). The samples were fresh-frozen or immersion fixed in either 10% neutral buffered formalin (NBF) or 70% ethyl alcohol plus 150 mM sodium chloride (EtOH), embedded in paraffin, and 6-μm-thick serial sections were cut.

Brains from nubian goats with a MPS IIID disorder (n = 4; 2 stillborn; one 19 month and one 25 month) and 2 normal goat brains were processed as described previously (45). Mice with MPS VII (n = 4) and unaffected mice (n = 7) were perfused transcardially with 4% paraformaldehyde plus chloral hydrate (52, 53) at 3 or 5 months of age and their brains were embedded in paraffin, and 6-μm-thick serial sections were cut. Two series of tissue sections were stained with hematoxylin and eosin and periodic acid-Schiff (PAS), respectively, to examine morphology. Deparaffinized tissue sections were blocked in 2% horse serum in Tris/HCl buffer (pH 7.6) for 1 h and incubated with primary antibodies (Table 2) in Tris buffer overnight at 4°C in a humidified chamber. Sections were processed with the ABC kit (Vector Labs, Burlingame, CA) and developed with 0.05% diaminobenzidine, 0.03% hydrogen peroxide, and 0.01 M imidazole in Tris buffer for 10 min (54, 55). For TS staining, deparaffinized tissue sections were immersed in 0.0125% TS (Sigma, St. Louis, MO) in a 40% ethanol/60% phosphate-buffered saline solution in the dark for 2 min. Tissue sections were visualized with a Nikon FXA photomicroscope equipped with epifluorescence and brightfield optics. For TS observation, a Nikon B-2E FITC filter was used. Microscope images were digitized to a computer workstation with image analysis software (Northern Exposure, Glen Mills, PA) and printed on a digital printer (Fuji, Japan) as described previously (54, 55).

For the ELISA assay, 2 extraction procedures were utilized to quantitate soluble and insoluble brain levels of Aβ (1-40) and Aβ (1-42). This ELISA assay does not cross react with APPs, and is specific for Aβ (1-40) and Aβ (1-42) (50). Soluble Aβ was measured from TBS extracted temporal neocortex, and

TABLE 2
Antibody Characterization

Antibody	Antigen	Species	Dilution	Reference	Source
2332	Aβ (1-10?)	rabbit	1:4,000	(82)	CNDR
6E10	Aβ (1-14)	mouse	1:700	(83)	Senetek
4G8	Aβ (16-20?)	mouse	1:2,000	(82)	Senetek
10D5	Aβ (1-28)	mouse	1:50	(84)	Athena
BA27	Aβ (1-40)	mouse	1:1,000	(49)	Takeda
BAN50	Aβ amino	mouse	1:1,000	(49)	Takeda
BC05	Aβ (1-42)	mouse	1:1,000	(49)	Takeda
654-39	rat Aβ (1-28)	rabbit	1:1,000	—	Athena
LN39	APP (1-100)	mouse	1:10	(85)	CNDR
10E4	HSGAG	mouse	1:100	(86)	U.S. Biological
3G10	HSPG	mouse	1:100	(86)	U.S. Biological
PHF6	tau pThr231	mouse	1:5,000	(87)	CNDR
T3P	tau Ser396	rabbit	1:50	(88)	CNDR

This table summarizes the antibodies (first column), antigen and corresponding epitope (question marks denote the approximate epitope) used for antibody generation (second column), species the antibody is raised in (third column), dilution used for immunohistochemistry (fourth column), citation of antibody characterization (fifth column), and source of the antibody (sixth column). The source denoted "CNDR" indicates the antibody was generated in the Center for Neurodegenerative Disease Research, University of Pennsylvania School of Medicine.

insoluble Aβ was assessed in formic acid extracted tissue homogenates. Briefly, 0.15 g cortex (with meninges stripped away) was Dounce-homogenized (20 strokes) in 4 ml of TBS (pH 7.4) or in 1 ml 70% formic acid with a protease inhibitor cocktail (1 μg/ml each in 5 mM EDTA: leupeptin, peptstatin A, soybean trypsin inhibitor, Nα-p-tosyl-L-lysine chloromethyl ketone [TLCK], and N-tosyl-L-phenylalanine chloromethyl ketone [TPCK]) at 4°C. All tissue homogenates were centrifuged at 125,000 g for 1 h at 4°C. Formic acid extracted samples were diluted 1:20 with 1 M Tris base. All samples were then diluted 1:2, 1:5, and 1:25 with EC buffer (20 mM sodium phosphate buffer pH 7.0, 2 mM EDTA, 400 mM NaCl, 0.2% bovine serum albumin, 0.05% CHAPS, 0.4% Block Ace [Snow Brand Milk Products, Sapporo, Japan], 0.05% NaN3, pH 7.0) prior to loading onto ELISA plates precoated with the capturing antibody BAN50 (Aβ amino-terminal specific) and reporter antibodies BA27 (Aβ [1-40] specific; 30 μg/ml) or BC05 (Aβ [1-42] specific; 15 μg/ml) for measurement as described previously (47–49). Statistical analyses consisted of analysis of variance (ANOVA) with post-hoc Neuman-Keuls test for significance.

RESULTS

MPS Cases

PAS staining revealed swollen neurons throughout the neuraxis in both the Hurler's (MPS I; n = 5) and Sanfilippo's (MPS III; n = 4) cases, consistent with previous observations (56–59). Moreover, the majority of neurons observed within these MPS brains contained abundant cytoplasmic HSPG immunoreactivity (Fig. 1A, D), demarcating perikaryal profiles distended with uncatabolized substrates as expected for MPS I and MPS III. In contrast, HSPG immunoreactivity was not abundant in the cytoplasmic domain of neurons in the brains of normal and disease control (AD, DS, NCL, and Gaucher) cases where HSPG immunoreactivity was localized principally to blood vessels and parenchymal surfaces (Fig. 1G). HSPG-immunoreactive NFTs and SPs were also observed in AD and DS brains (Fig. 1G), but not in MPS, NCL, or Gaucher brains.

TS staining revealed no NFTs or SPs within the MPS brains, but intensely autofluorescent, punctate lipid accumulations were observed in the cytoplasm of neurons throughout cortical and subcortical regions (data not shown), consistent with previous observations (56, 60, 61). Little or no PHFtau immunoreactivity was detected in the brains of the 9 MPS cases (Fig. 1B, E). Robust PHFtau-immunoreactive NFTs, neuropil threads, and dystrophic neurites were observed, however, in AD and DS cases processed in parallel with the MPS cases (Fig. 1H). Immunohistochemistry using antibodies directed against Aβ peptides did not reveal extracellular SPs within the brains of the MPS cases. However, abundant intracellular Aβ immunoreactivity was detected in the MPS brains, notably within the somatodendritic domain of neurons within the neocortex and hippocampal formation (Figs. 1C, F, 2A–C).

Neither intracellular Aβ immunoreactivity or SPs were observed in the brains of NCL or Gaucher's disease patients. By using a panel of MAbs and polyclonal antibodies specific for several different epitopes within Aβ (Table 2), we were able to determine that Aβ (1-40) immunoreactivity was the most abundant species in intracellular stores in MPS brains. In contrast, antibodies specific for Aβ (1-42) did not reveal intracellular labeling in the MPS brains. Qualitatively, cytoplasmic Aβ (1-40)

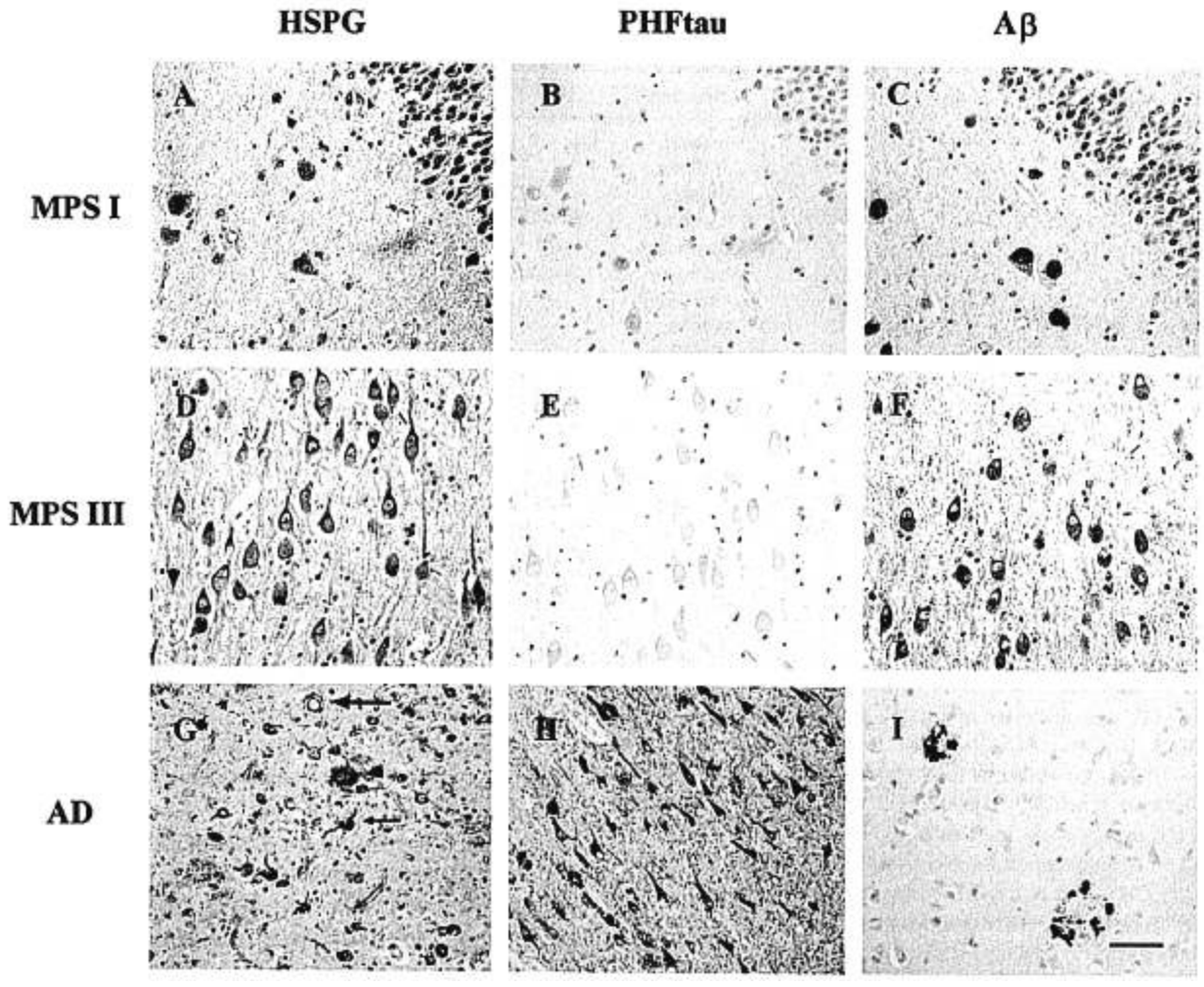

Fig. 1. Differential distribution of HSPG, PHFtau, and Aβ immunoreactivity within MPS and AD brains. Sections (A–I) are counterstained with hematoxylin. All panels are at the same magnification and the scale bar in I = 30 μm. A: HSPG immunoreactivity within the granule cell layer of the dentate gyrus and hippocampal hilus of an MPS I (Hurler's syndrome) brain. Cytoplasmic HSPG immunoreactivity delineates swollen storage neurons. B: Adjacent section to (A), stained with an antibody directed against PHFtau. Note the paucity of cellular staining within the hippocampal formation. C: Adjacent section to (B), stained with an antibody directed against Aβ peptides. Abundant cytoplasmic labeling is detected within the granule cell layer and hilar neurons, similar to observations with HSPG immunoreactivity. D: HSPG immunoreactivity within CA1 subfield of the hippocampus of an MPS III (Sanfilippo's syndrome) brain. Similar to (A), abundant cytoplasmic labeling of neurons is observed. E: A paucity of PHFtau immunoreactivity is observed in a tissue section adjacent to (D). F: Aβ-immunoreactive neurons throughout the CA1 subfield in a tissue section adjacent to (E). Similar to (C), abundant cytoplasmic labeling of intracellular Aβ peptides is detected in the MPS III brain. G: HSPG immunoreactivity within the CA1-subicular region of an AD brain. HSPG-immunoreactive blood vessels (thick arrow), SPs (arrowhead), and NFTs (thin arrow) are observed within this field. H: PHFtau-immunoreactive NFTs and neuropil threads are observed within the CA1 region. I: Two Aβ-immunoreactive SPs are observed within the CA1-subiculum, with little or no intracellular Aβ immunoreactivity within neuronal profiles.

immunoreactivity appeared similar in staining intensity and distribution to HSPG immunoreactivity within neurons of the MPS brains. In contrast, Aβ-immunoreactive SPs were observed within the brains of AD and DS cases, with relatively little intracellular Aβ immunoreactivity detected in neurons (Fig. 1I).

ELISA assays using an amino-terminal capturing antibody and end-specific Aβ reporter MAbs combined with TBS extracted soluble and formic acid extracted insoluble temporal cortex tissue homogenates detected both Aβ (1-40) and Aβ (1-42) in CTR, MPS, and AD brains. Although the total amount of Aβ peptides quantitated in MPS and CTR brains was low, we detected a statistically significant ($p < 0.001$), 3-fold increase in the amount of soluble Aβ (1-40) in the MPS temporal cortex homogenates compared with CTR homogenates (0.92 ± 0.05 (sem) pmol/g wet tissue vs 0.30 ± 0.03 pmol/g wet tissue; Fig. 3A). No significant differences were found between MPS and CTR homogenates for insoluble Aβ (1-40) (0.28 ± 0.03 pmol/g wet tissue vs

Fig. 2. Detection of intracellular Aβ immunoreactivity in MPS brains. Sections are counterstained with hematoxylin. All panels are at the same magnification and the scale bar in C = 10 μm. A: Aβ-immunoreactive granule cells from a MPS I brain. B: Perinuclear, somatodendritic Aβ immunoreactivity is observed in CA1 neurons from the same MPS I brain as (A). C: Punctate, Aβ-immunoreactive labeling of pyramidal cells from temporal neocortex of an MPS III brain further illustrate cytoplasmic storage accumulations in these neurons.

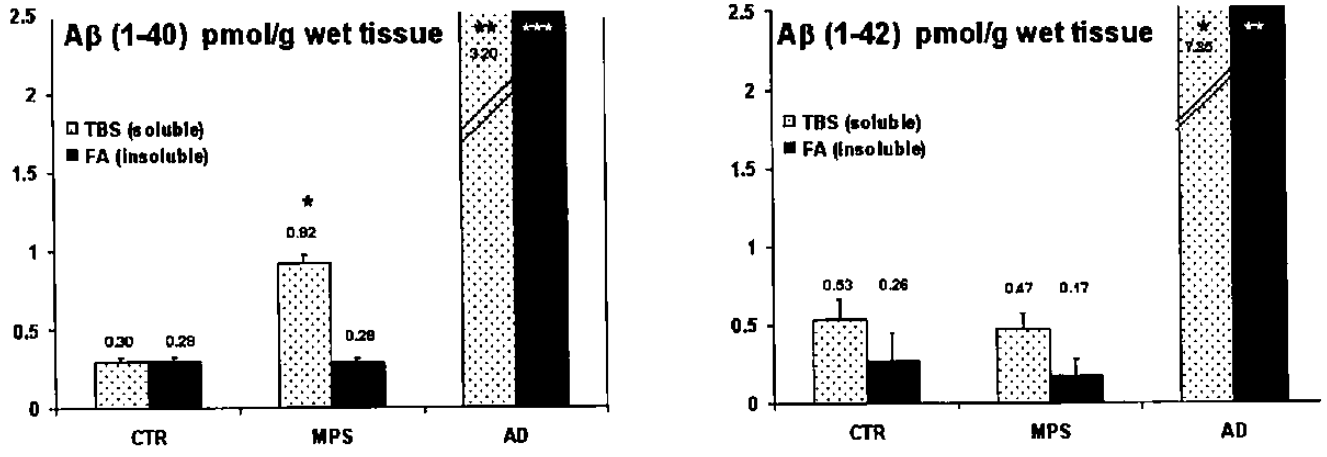

Fig. 3. Quantitation of soluble and insoluble Aβ (1-40) and Aβ (1-42) obtained from temporal neocortex of CTR, MPS, and AD brains using a sensitive two-site sandwich ELISA with end-specific monoclonal Aβ antibodies. Results are reported in units of pmol/g wet tissue for soluble (Tris-buffered saline [TBS] extracted; gray shading) and insoluble (formic acid [FA] extracted; black shading) Aβ (1-40) and Aβ (1-42). The scale for the AD homogenates has been split (hatched lines) to reflect that the actual values are larger than the *y*-axis scale. A: Although the total abundance of Aβ peptides is low in MPS brains, a 3-fold increase in soluble Aβ (1-40) was observed in the MPS homogenates as compared with CTR homogenates (asterisk; $p < 0.001$). No differences were observed between MPS and CTR brains for insoluble Aβ (1-40). As a positive control, soluble Aβ (1-40) (double asterisk; $p < 0.0001$) and insoluble Aβ (1-40) (white triple asterisk; $p < 0.00001$) were significantly elevated in AD homogenates. B: No significant differences were observed between MPS and CTR homogenates for soluble or insoluble Aβ (1-42). In contrast, significant elevations in both soluble Aβ (1-42) (single asterisk; $p < 0.0001$) and insoluble (1-42) (double white asterisk; $p < 0.00001$) were found for AD homogenates.

0.29 ± 0.03 pmol/g wet tissue). In addition, no differences were detected between MPS and CTR homogenates by ELISA for either soluble or insoluble Aβ (1-42) (Fig. 3B). To further validate the efficacy of the Aβ ELISA assay, homogenates obtained from the temporal neocortex of AD patients were used as a positive control. Similar to previous reports (47, 50), both soluble and insoluble Aβ (1-40) and Aβ (1-42) were elevated in AD temporal neocortex homogenates compared with CTR homogenates.

In addition, abundant cytoplasmic APP immunoreactivity was detected within neurons in the MPS brains (Fig. 4A–D), within neurons, NFTs, neuropil threads, SP cores in AD and DS brains (Fig. 4E, F), and within neurons in control brains (not shown). In summary, HSPG, PHFtau, Aβ, and APP immunoreactivity were similar in expression, distribution, and staining intensity in both MPS I and MPS III brains, and the expression of HSPG and Aβ differed from those observed in CTR, AD, and DS brains.

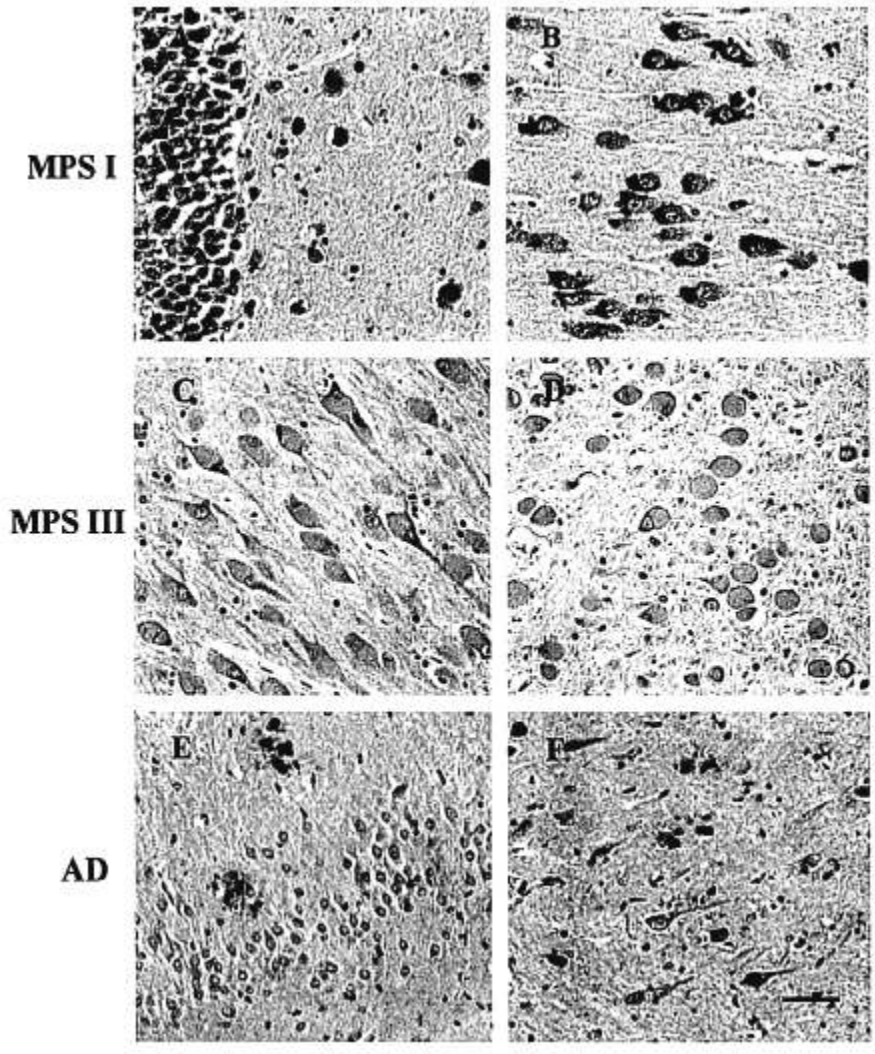

Fig. 4. Differential distribution of APP immunoreactivity within MPS and AD brains. Sections are counterstained with hematoxylin. All panels are at the same magnification and the scale bar in F = 30 μm. A, B: Abundant perinuclear, cytoplasmic APP immunoreactivity is detected in granule cells and hilar neurons (A) and temporal neocortex (B) of an MPS I brain. C, D: Neuronal APP immunoreactivity observed within the CA1 region (C) and temporal neocortex (D) of an MPS III brain. E, F: Moderate cytoplasmic APP labeling of neurons is observed in an AD brain. APP-immunoreactive SP cores within the hilar region (E) and APP-immunoreactive NFTs and dystrophic processes within temporal neocortex (F) display intense labeling.

Murine and Caprine Models of MPS

PAS staining revealed swollen neurons within the brains of both MPS IIID goats and MPS VII mice similar to previous observations (45, 52, 53). Cytoplasmic HSPG immunoreactivity was abundant in the goat MPS IIID brains (Fig. 5A), similar to the human MPS cases. In contrast, moderate to weak HSPG immunoreactivity was observed in the murine MPS VII cases and unaffected goat controls (Fig. 5D). TS staining of brain sections from MPS IIID goats and MPS VII mice did not reveal NFTs or SPs, and there was no intracytoplasmic PHFtau immunoreactivity in either of the caprine or murine MPS models (Fig. 5B, E). Intracellular accumulation of Aβ immunoreactivity within neurons was observed in the MPS IIID goat brains, similar to the human MPS cases (Fig. 5C) but not in the unaffected caprine controls. In contrast to the MPS IIID goats, MPS VII mouse brains did not display abundant Aβ immunoreactivity (Fig. 5F), even when antibodies directed against rat Aβ (1–28) were used.

DISCUSSION

The neuropathology of MPS I (Hurler's syndrome) and MPS III (A–D) (Sanfilippo's syndrome) has been well described in extensive detail (56–59). However, evidence of PHFtau and Aβ pathology within the MPS brain has not been reported previously. Because GAGs, notably HSGAGs, have been shown by several criteria to be potential pathological chaperones in the formation of tau-positive PHFs and Aβ-containing SPs (27–29, 31, 37,

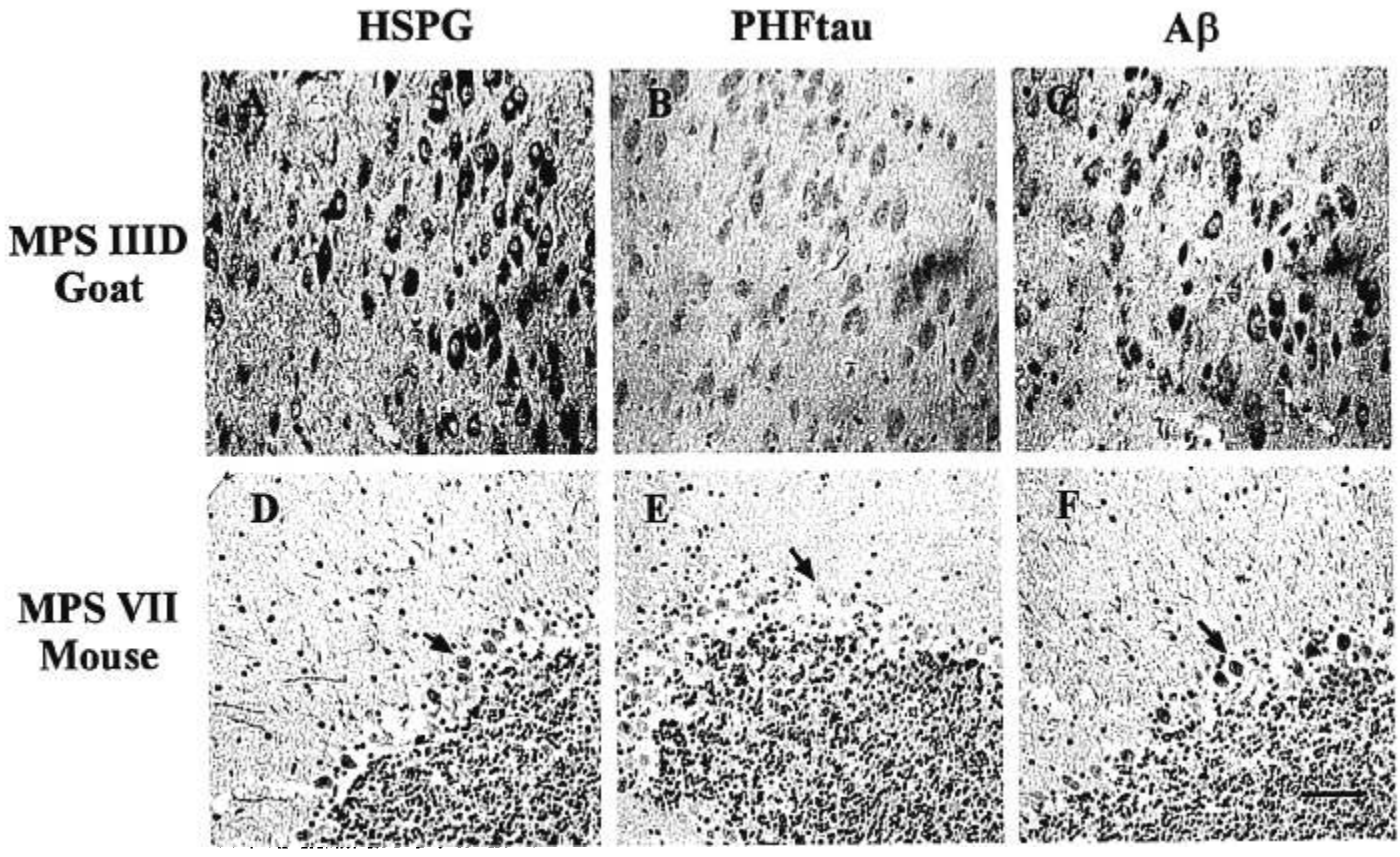

Fig. 5. Distribution of HSPG, PHFtau, and Aβ immunoreactivity within the brains of caprine (A–C) and murine (D–F) MPS models. Sections are counterstained with hematoxylin. All panels are at the same magnification and the scale bar in F = 30 μm. A: Tissue section from the CA1 region of hippocampus of an MPS IIID goat stained with an antibody directed against HSPG. Note the intense perinuclear, somatodendritic labeling similar to human MPS cases. B: Adjacent section to (A), illustrating the paucity of PHFtau immunostaining. C: Adjacent section to (B), demonstrating strong to moderate Aβ immunoreactivity. D: Tissue section from the cerebellum of an MPS VII mouse stained with an antibody directed against HSPG. Moderate to weak HSPG immunoreactivity is detected within Purkinje cell bodies (arrow) and dendrites, and contrasts the intense HSPG immunoreactivity observed in the MPS IIID goat brains. E: Adjacent section to (D), demonstrating a lack of PHFtau immunoreactivity (arrow). F: Adjacent section to (E), illustrating moderate to weak Aβ immunoreactivity within Purkinje cells (arrow).

39), we hypothesized that accumulations of uncatabolized HSGAGs in MPS brains due to lysosomal enzyme deficiencies could induce the formation of NFTs and SPs. Notwithstanding, SPs and NFTs are typically associated with progressive, late-onset disorders such as AD, and the majority of MPS patients die before AD typically begins (43, 44), SPs have been observed in the brains of some adolescent DS patients (62, 63), and in most DS patients surviving past the third decade of life (64). In addition, NFTs are observed in the brains of adolescents with subacute sclerosing panencephalitis (65–67), as well as in the brains of adolescent patients with Niemann-Pick type C disease, a cholesterol storage disorder (68–70). Thus, even though NFT and SP pathology was not observed by TS and immunohistochemistry for PHFtau and Aβ peptides in the present set of MPS cases (ages 1–42 years), tangle and plaque pathology has been observed (albeit rarely) in patients with other disorders who were as young as the MPS patients in the present report.

The detection of intense and diffuse APP and increased Aβ (1-40) immunoreactivity within the cytoplasm of neurons throughout MPS brains is intriguing because insights into this phenomenon may clarify mechanisms of amyloidosis in AD. For example, it will be important to determine if uncatabolized accumulation of HSGAGs in MPS syndromes lead to an increase in the synthesis of soluble Aβ, or a decrement in the secretion or degradation of Aβ. Three pathways have been identified in the proteolytic processing of APPs into Aβ peptides, including an endoplasmic reticulum/intermediate compartment pathway that generates principally Aβ (1-42) species (71–73), a trans-Golgi network pathway that generates Aβ (1-40) (major species) and Aβ (1-42) species (74, 75), and an endosomal/lysosomal pathway that also generates secreted Aβ (1-40) (major species) and Aβ (1-42) (76–79). The latter pathway may be most relevant in MPS, because APP and Aβ, like HSGAGs, are degraded (or recycled) in part by an endosomal-lysosomal pathway

(76, 77, 79). Moreover, GAGs, including HSGAG, have been reported to inhibit (>20) lysosomal glycolipid and acid hydrolases (80, 81). Thus, overall lysosomal efficiency may be compromised in MPS, and the accumulation of uncatabolized HSGAGs may impair the degradation of many macromolecules that are normally proteolyzed within these organelles, including APP and/or Aβ peptides.

This is the first report of robust intraneuronal Aβ (1-40) immunoreactivity in the human MPS brain or the brain of an experimental animal model of MPS. Thus, our findings here provide in vivo support for in vitro studies demonstrating that Aβ peptides accumulate within the cytoplasm of cultured cells, especially cells overexpressing neuron-predominant APP695 constructs (48, 72, 73). Moreover, studies of intracellular trafficking and processing of Aβ peptides leading to increased intracellular levels of Aβ (1-40) versus Aβ (1-42) linked to the lysosomal storage defects in MPS may provide insights in to mechanisms of amyloidosis in AD. We hypothesize that the lack SPs observed in MPS brains may be associated with the lack of increased levels of Aβ (1-42), which has a higher propensity to form insoluble aggregates compared with Aβ (1-40). Because heparin binding domains have been detected in APPs and HSPGs interact directly with Aβ peptides (28, 30, 40–42), the intracellular Aβ immunoreactivity in MPS brains leads to the speculation that a pathological increase in intracellular HSPGs due to MPS may promote interactions between HSPGs and Aβ peptides that lead to accumulations of these peptides within the somatodendritic domain.

In addition to human MPS brains, we also studied the brains of 2 animal models of HSGAG accumulation. MPS IIID goats accumulate HSPGs and the neuropathology of this model is well characterized (45), but it does not include NFTs and SPs. However, the caprine MPS IIID brain does show intracellular Aβ accumulations and little or no PHFtau immunoreactivity, similar to our observations in the human MPS I and MPS III brains. Thus, this is an excellent animal model to probe the basis of HSGAG overexpression-Aβ peptide interactions. The murine MPS VII model also has well-characterized neuropathological changes (46), but no NFTs and SPs. The mouse MPS VII model has many experimental advantages, including potential amelioration of storage deficiencies by transplantation or somatic gene transfer (52, 53), however, the moderate to weak expression of HSPG (as other uncatabolized GAGs, such as chondroitin sulfate and dermatan sulfate accumulate in MPS VII) and Aβ immunoreactivity does not recapitulate our human MPS I and MPS III observations. Moreover, it would be relevant now to determine if other mouse or large animal models (transgenic and spontaneous mutations) of MPS might be suitable for studies of GAG/Aβ interactions.

In conclusion, the lack of plaque and tangle pathology in the presence of in vivo HSGAG accumulation does not exclude the possibility that GAGs (notably the highly sulfated heparin and HSPG) may serve as pathological chaperones for PHF formation and amyloidosis as demonstrated by several groups in vitro (25, 27, 32, 37). Rather, our findings suggest that complex interactions of genetic, developmental, and environmental factors contribute to the accumulation of insoluble filaments in the form of NFTs, dystrophic processes, and SPs. Moreover, the observation that intracellular soluble Aβ (1-40) is increased in the diseases studied here implies that deficits in lysosomal degradation and subsequent accumulations of HSGAGs may cause an increase in APP and/or Aβ in the cytoplasm of storage neurons. Thus, MPS patient samples and MPS animal models may enable mechanistic studies of the role of Aβ peptides and HSPGs/HSGAGs in the amyloidosis that characterizes AD.

ACKNOWLEDGMENTS

We thank Dr. E.A. Alvord Jr., and Dr. A. Skorupa for tissue procurement, Dr. J. Wang and S. Leight for assistance with the ELISA assay, and T-S. Chiu and A. Polesky for technical assistance.

REFERENCES

1. Ginsberg SD, Schmidt ML, Crino PB, Eberwine JH, Lee VM-Y, Trojanowski JQ. Molecular pathology of Alzheimer's disease and related disorders. In: Peters A, Morrison JH, eds. Cerebral Cortex, vol. 14. Neurodegenerative and age-related changes in structure and function of cerebral cortex. New York: Plenum Press, 1999:603–53
2. Wasco W, Tanzi R Molecular mechanisms of dementia. Totowa, New Jersey: Humana Press, 1996
3. Goedert M, Trojanowski JQ, Lee M-Y. The neurofibrillary pathology of Alzheimer's disease. In: Rosenberg RN, Prusiner SB, DiMauro S, Barchi RL, eds. The molecular and genetic basis of neurological disease. Second Edition. Boston: Butterworth-Heinemann, 1997:613–27
4. Crowther RA, Wischik CM. Image reconstruction of the Alzheimer paired helical filament. Embo J 1985;4:3661–65
5. Goedert M, Wischik CM, Crowther RA, Walker JE, Klug A. Cloning and sequencing of the cDNA encoding a core protein of the paired helical filament of Alzheimer disease: Identification as the microtubule-associated protein tau. Proc Natl Acad Sci USA 1988;85:4051–55
6. Kondo J, Honda T, Mori H, et al. The carboxyl third of tau is tightly bound to paired helical filaments. Neuron 1988;1:827–34
7. Kosik KS, Joachim CL, Selkoe DJ. Microtubule-associated protein tau is a major antigenic component of paired helical filaments in Alzheimer's disease. Proc Natl Acad Sci USA 1986;83:4044–48
8. Kosik KS, Orecchio LD, Binder L, Trojanowski JQ, Lee VM-Y, Lee G. Epitopes that span the tau molecule are shared with paired helical filaments. Neuron 1988;1:817–25
9. Lee VM-Y, Balin BJ, Otvos Jr. L, Trojanowski JQ. A68: a major subunit of paired helical filaments and derivatized forms of normal tau. Science 1991;251:675–78
10. Wischik CM, Novak M, Thogersen HC, et al. Isolation of a fragment of tau derived from the core of the paired helical filament of Alzheimer's disease. Proc Natl Acad Sci USA 1988;85:4506–10

11. Ksiezak-Reding H, Yen SH. Structural stability of paired helical filaments requires microtubule-binding domains of tau: A model for self association. Neuron 1991;6:717–28
12. Crowther RA, Olesen OF, Jakes R, Goedert M. The microtubule binding repeats of tau protein assemble into filaments like those found in Alzheimer's disease. FEBS Lett 1992;309:199–202
13. Trojanowski JQ, Clark CM, Schmidt ML, et al. Implications of tau-rich neurofibrillary lesions for the pathobiology and diagnosis of Alzheimer's disease. In: Appell SH, ed. Current Neurology, Vol. 16. Boston: Houghton Mifflin, 1996:93–113
14. Glenner GG, Wong CW. Alzheimer's disease: Initial report of the purification and characterization of a novel cerebrovascular amyloid protein. Biochem Biophys Res Commun 1984;120:885–90
15. Masters CL, Simms G, Weinman NA, Multhaup G, McDonald BL, Beyreuther K. Amyloid plaque core protein in Alzheimer disease and Down syndrome. Proc Natl Acad Sci USA 1985;82:4245–49
16. Burdick D, Soreghan B, Kwon M, et al. Assembly and aggregation properties of synthetic Alzheimer's A4/β amyloid peptide analogs. J Biol Chem 1992;267:546–54
17. Halverson K, Fraser PE, Kirschner DA, Lansbury PT. Molecular determinants of amyloid deposition in Alzheimer's disease: Conformational studies of synthetic β-protein fragments. Biochemistry 1990;29:4108–16
18. Naiki H, Nakakuki K. First-order kinetic model of Alzheimer's β-amyloid fibril extension in vitro. Lab Invest 1996;74:374–83
19. Levine H, III. Thioflavine T interaction with synthetic Alzheimer's disease β-amyloid peptides: Detection of amyloid aggregation in solution. Prot Sci 1993;2:404–10
20. Kirschner DA, Inouye H, Duffy LK, Sinclair A, Lind M, Selkoe DJ. Synthetic peptide homologous to β protein from Alzheimer disease forms amyloid-like fibrils in vitro. Proc Natl Acad Sci USA 1987;84:6953–57
21. Yang AJ, Knauer M, Burdick DA, Glabe C. Intracellular Aβ 1-42 aggregates stimulate the accumulation of stable, insoluble amyloidogenic fragments of the amyloid precursor protein in transfected cells. J Biol Chem 1995;270:14786–92
22. Iwatsubo T, Okada A, Suzuki N, Mizusawa H, Nukina N, Ihara Y. Visualization of Aβ42(43) and Aβ40 in senile plaques with end-specific Aβ monoclonals: Evidence that an initially deposited species is Aβ42(43). Neuron 1994;13:45–53
23. Iwatsubo T, Mann DMA, Odaka A, Suzuki N, Ihara Y. Amyloid-β protein (Aβ) deposition: Aβ42(43) precedes Aβ40 in Down's syndrome. Ann Neurol 1995;37:294–99
24. Roher AE, Lowenson JD, Clarke S, et al. Structural alterations in the peptide backbone of β-amyloid core protein may account for its deposition and stability in Alzheimer's disease. J Biol Chem 1993;268:3072–83
25. Arrasate M, Perez M, Valpuesta JM, Avila J. Role of glycosaminoglycans in determining the helicity of paired helical filaments. Am J Pathol 1997;151:1115–22
26. Friedhoff P, von Bergen M, Mandelkow E-M, Davies P, Mandelkow E. A nucleated assembly mechanism of Alzheimer paired helical filaments. Proc Natl Acad Sci USA 1998;95:15712–17
27. Goedert M, Jakes R, Spillantini MG, Hasegawa M, Smith MJ, Crowther RA. Assembly of microtubule-associated protein tau into Alzheimer-like filaments induced by sulfated glycosaminoglycans. Nature 1996;383:550–53
28. Castillo GM, Ngo C, Cummings J, Wight TN, Snow AD. Perlecan binds to the amyloid-β proteins (Aβ) of Alzheimer's disease, accelerates Aβ fibril formation, and maintains Aβ fibril stability. J Neurochem 1997;69:2452–65
29. Perry G, Siedlak SL, Richey P, et al. Association of heparan sulfate proteoglycan with the neurofibrillary tangles of Alzheimer's disease. J Neurosci 1991;11:3679–83
30. Snow AD, Sekiguchi R, Nochlin D, et al. An important role of heparan sulfate proteoglycan (Perlecan) in a model system for the deposition and persistence of fibrillar Aβ-amyloid in rat brain. Neuron 1994;12:219–34
31. Su JH, Cummings BJ, Cotman CW. Localization of heparan sulfate glycosaminoglycan and proteoglycan core protein in aged brain and Alzheimer's disease. Neuroscience 1992;51:801–13
32. Hasegawa M, Crowther RA, Jakes R, Goedert M. Alzheimer-like changes in microtubule-associated protein tau induced by sulfated glycosaminoglycans. Inhibition of microtubule binding, stimulation of phosphorylation, and filament assembly depend of the degree of sulfation. J Biol Chem 1997;273:33118–24
33. Salmivirta M, Lidholt K, Lindahl U. Heparan sulfate: A piece of information. FASEB J 1996;10:1270–79
34. Kjellen L, Lindahl U. Proteoglycans: Structures and interactions. Ann Rev Biochem 1991;60:443–75
35. Brandt R, Lee G, Teplow DB, Shalloway D, Abdel-Ghany M. Differential effect of phosphorylation and substrate modulation on tau's ability to promote microtubule growth and nucleation. J Biol Chem 1994;269:11776–82
36. Yang SD, Yu JS, Shiah SG, Huang JJ. Protein kinase FA/glycogen synthase kinase-3 alpha after heparin potentiation phosphorylates tau on sites abnormally phosphorylated in Alzheimer's disease brain. J Neurochem 1994;63:1416–25
37. Perez M, Valpuesta JM, Medina M, Montejo de Garcini E, Avila J. Polymerization of tau into filaments in the presence of heparin: The minimal sequence required for tau-tau interaction. J Neurochem 1996;67:1183–90
38. Snow AD, Mar H, Nochlin D, et al. The presence of heparan sulfate proteoglycans in the neuritic plaques and congophilic angiopathy in Alzheimer's disease. Am J Pathol 1988;133:456–63
39. Snow AD, Wight TN. Proteoglycans in the pathogenesis of Alzheimer's disease and other amyloidoses. Neurobiol Aging 1989;10:481–97
40. Buee L, Ding W, Delacourte A, Fillit H. Binding of secreted human neuroblastoma proteoglycans to the Alzheimer's amyloid A4 peptide. Brain Res 1993;601:154–63
41. Fraser PE, Nguyen JT, Chin DT, Kirschner DA. Effects of sulfate ions on Alzheimer β/A4 peptide assemblies: Implications for amyloid fibril-proteoglycan interactions. J Neurochem 1992;59:1531–40
42. Narindrasorasak S, Lowery D, Gonzalez-DeWhitt P, Poorman RA, Greenberg B, Kisilevsky R. High affinity interactions between the Alzheimer's β-amyloid precursor proteins and the basement membrane form of heparan sulfate proteoglycan. J Biol Chem 1991;266:12878–83
43. Hopwood JJ, Morris CP. The mucopolysaccharidoses. Diagnosis, molecular genetics and treatment. Mol Biol Med 1990;7:381–404
44. Neufeld EF, Muenzer M. The mucopolysaccharidoses. In: Scriver CR, Beaudet AL, Sly WS, Valle D, eds. The metabolic and molecular bases of inherited disease, 7th Edition. New York: McGraw-Hill, 1995:2465–94
45. Jones MZ, Alroy J, Boyer PJ, et al. Caprine mucopolysaccharidosis-IIID: Clinical, biochemical, morphological, and immunohistochemical characteristics. J Neuropathol Exp Neurol 1998;57:148–57
46. Levy B, Galvin N, Vogler C, Birkenmeier EH, Sly WS. Neuropathology of murine mucopolysaccharidosis type VII. Acta Neuropathol 1996;92:562–68
47. Hosoda R, Saido TC, Otvos J, L., et al. Quantification of modified amyloid β peptides in Alzheimer disease and Down syndrome brains. J Neuropathol Exp Neurol 1998;57:1089–95
48. Skovronsky DM, Doms RW, Lee VM-Y. Detection of a novel intraneuronal pool of insoluble amyloid β protein that accumulates with time in culture. J Cell Biol 1998;141:1031–39
49. Suzuki N, Cheung TT, Cai XD, et al. An increased percentage of long amyloid-β protein secreted by familial amyloid-β protein precursor (βAPP717) mutants. Science 1994;264:1336–40

50. Wang J, Dickson DW, Trojanowski JQ, Lee VM-Y. The levels of soluble versus insoluble brain Aβ distinguish Alzheimer's disease from normal and pathologic aging. Exp Neurol 1999 (in press)
51. Turner RS, Suzuki N, Chyung ASC, Younkin SG, Lee VM-Y. Amyloids β40 and β42 are generated intracellularly in cultured human neurons and their secretion increases with maturation. J Biol Chem 1996;271:8966–70
52. Snyder EY, Taylor RM, Wolfe JH. Neural progenitor cell engraftment corrects lysosomal storage throughout the MPS VII mouse brain. Nature 1995;374:367–70
53. Wolfe JH, Sands MS, Barker JE, et al. Reversal of pathology in murine mucopolysaccharidosis type VII by somatic cell gene transfer. Nature 1992;360:749–53
54. Ginsberg SD, Crino PB, Lee VM-Y, Eberwine JH, Trojanowski JQ. Sequestration of RNA in Alzheimer's disease neurofibrillary tangles and senile plaques. Ann Neurol 1997;41:200–209
55. Galvin JE, Lee VM-Y, Baba M, et al. Monoclonal antibodies to purified cortical Lewy bodies recognize the mid-size neurofilament subunit. Ann Neurol 1997;42:595–603
56. Jones MZ, Alroy J, Rutledge JC, et al. Human mucopolysaccharidosis IIID. Clinical, biochemical, morphological, and immunohistochemical characteristics. J Neuropathol Exp Neurol 1997;56: 1158–67
57. Dekaban AS, Constantopoulos G. Mucopolysaccharidosis types I, II, IIIA, and V. Pathological and biochemical abnormalities in the neural and mesenchymal elements of the brain. Acta Neuropathol 1977;39:1–7
58. Ghatak NR, Fleming DF, Hinman A. Neuropathology of Sanfilippo syndrome. Ann Neurol 1977;2:161–66
59. Hadfield MG, Ghatak NR, Nakoneczna I, et al. Pathologic findings in mucopolysaccharidosis type IIIB (Sanfilippo's syndrome B). Arch Neurol 1980;37:645–50
60. Dowson JH, Wilton-Cox H, Oldfors A, Sourander P. Autofluorescence emission spectra of neuronal lipopigment in mucopolysaccharidosis (Sanfilippo's syndrome). Acta Neuropathol 1989;77:426–29
61. Oldfors A, Sourander P. Storage of lipofuscin in neurons in mucopolysaccharidosis. Report on a case of Sanfilippo's syndrome with histochemical and electron-microscopic findings. Acta Neuropathol 1981;54:287–92
62. Lemere CA, Blusztajn JK, Yamaguchi H, Wisniewski T, Saido TC, Selkoe DJ. Sequence of deposition of heterogeneous amyloid β-peptides and APO E in Down syndrome: Implications for initial events in amyloid plaque formation. Neurobiol Disease 1996;3:16–32
63. Leverenz JB, Raskind MA. Early amyloid deposition in the medial temporal lobe of young Down syndrome patients: A regional quantitative analysis. Exp Neurol 1998;150:296–304
64. Wisniewski KE, Dalton AJ, Crapper McLachlan DR, Wen GY, Wisniewski HM. Alzheimer's disease in Down's syndrome: Clinicopathologic studies. Neurology 1985;35:957–61
65. Mandybur TI, Nagpaul AS, Pappas Z, Niklowitz WJ. Alzheimer neurofibrillary change in subacute sclerosing panencephalitis. Ann Neurol 1977;1:103–7
66. McQuaid S, Kirk J, Zhou AL, Allen IV. Measles virus infection of cells in perivascular infiltrates in the brain in subacute sclerosing panencephalitis: Confirmation by non-radioactive in situ hybridization, immunocytochemistry and electron microscopy. Acta Neuropathol 1993;85:154–58
67. McQuaid S, Allen IV, McMahon J, Kirk J. Association of measles virus with neurofibrillary tangles in subacute sclerosing panencephalitis: A combined in situ hybridization and immunocytochemical investigation. Neuropathol Appl Neurobiol 1994;20:103–10
68. Auer IA, Schmidt ML, Lee VM-Y, et al. Paired helical filament tau (PHFtau) in Niemann-Pick type C disease is similar to PHFtau in Alzheimer's disease. Acta Neuropathol 1995;90:547–51
69. Love S, Bridges LR, Case CP. Neurofibrillary tangles in Niemann-Pick disease type C. Brain 1995;118:119–29
70. Suzuki K, Parker CC, Pentchev PG, et al. Neurofibrillary tangles in Niemann-Pick disease type C. Acta Neuropathol 1995;89:227–38
71. Chyung ASC, Greenberg BD, Cook DG, Doms RW, Lee VM-Y. Novel β-secretase cleavage of β-amyloid precursor protein in the endoplasmic reticulum/intermediate compartment of NT2N cells. J Cell Biol 1997;138:671–80
72. Cook DG, Forman M, Sung JC, et al. Alzheimer's Aβ(1-42) is generated in the endoplasmic reticulum/intermediate compartment of NT2N cells. Nat Med 1997;3:1021–23
73. Hartmann T, Bieger SC, Bruhl B, et al. Distinct sites of intracellular production for Alzheimer's disease Aβ40/42 amyloid peptides. Nat Med 1997;3:1016–20
74. Greenfield JP, Tsai J, Gouras GK, et al. Endoplasmic reticulum and trans-Golgi network generate distinct populations of Alzheimer β-amyloid peptides. Proc Natl Acad Sci USA 1999;96:742–47
75. Xu H, Sweeney D, Wang R, et al. Generation of Alzheimer β-amyloid protein in the trans-Golgi network in the apparent absence of vesicle formation. Proc Natl Acad Sci USA 1997;94:3748–52
76. Koo EH, Squazzo SL. Evidence that production and release of amyloid β-protein involves the endocytic pathway. J Biol Chem 1994;269:17386–89
77. Koo EH, Squazzo SL, Selkoe DJ, Koo CH. Trafficking of cell-surface amyloid β-protein precursor. I. Secretion, endocytosis and recycling as detected by labeled monoclonal antibody. J Cell Sci 1996;109:991–98
78. Haass C, Koo EH, Mellon A, Hung AY, Selkoe DJ. Targeting of cell-surface β-amyloid precursor protein to lysosomes: Alternative processing into amyloid-bearing fragments. Nature 1992;357:500–503
79. Yamazaki T, Koo EH, Selkoe DJ. Trafficking of cell-surface amyloid β-protein precursor. II. Endocytosis, recycling and lysosomal targeting detected by immunolocalization. J Cell Sci 1996;109: 999–1008
80. Baumkötter J, Cantz M. Decreased ganglioside neuraminidase activity in fibroblasts from mucopolysaccharidosis patients. Inhibition of the activity in vitro by sulfated glycosaminoglycans and other compounds. Biochem Biophys Acta 1983;761:163–70
81. Avila JL, Convit J. Inhibition of leucocytic lysosomal enzymes by glycosaminoglycans. Biochem J 1975;152:57–64
82. Schmidt ML, DiDario AG, Otvos Jr. L, et al. Plaque-associated neuronal proteins: a recurrent motif in neuritic amyloid deposits throughout diverse cortical areas of the Alzheimer's disease brain. Exp Neurol 1994;130:311–22
83. Kim KS, Miller DL, Sapienza VJ, et al. Production and characterization of monoclonal antibodies reactive to synthetic cerebrovascular amyloid peptide. Neurosci Res Commun 1988;2:121–30
84. Hyman BT, Tanzi RE, Marzloff K, Barbour R, Schenk D. Kunitz protease inhibitor-containing amyloid-β protein precursor immunoreactivity in Alzheimer's disease. J Neuropathol Exp Neurol 1992;51:76–83
85. Arai H, Lee VM-Y, Messinger ML, Greenberg BD, Lowery DE, Trojanowski JQ. Expression patterns of β-amyloid precursor protein (β-APP) in neural and noneural human tissues from Alzheimer's disease and control subjects. Ann Neurol 1991;30:686–93
86. David G, Bai XM, Van der Schueren B, Cassiman JJ, Van den Berghe H. Developmental changes in heparan sulfate expression: In situ detection with mAbs. J Cell Biol 1992;119:961–75
87. Hoffmann R, Lee VM-Y, Leight S, Varga I, Otvos L, Jr. Unique Alzheimer's disease paired helical filament specific epitopes involve double phosphorylation at specific sites. Biochem 1997;36:8114–24
88. Bramblett GT, Goedert M, Jakes R, Merrick SE, Trojanowski JQ, Lee VM-Y. Abnormal tau phosphorylation at Ser 396 in Alzheimer's disease recapitulates development and contributes to reduced microtubule binding. Neuron 1993;10:1089–99

Received February 1, 1999
Revision received April 2, 1999
Accepted April 5, 1999